Journal of Experimental Botany, Vol. 49, No. 323, pp. 953–965, June 1998

Journal of Experimental Botany

Tissue localization of phenolic compounds in plants by confocal laser scanning microscopy

Peter Hutzler[1], Robert Fischbach[2], Werner Heller[3], Tim P. Jungblut[3], Sebastian Reuber[4], Rainer Schmitz[4], Markus Veit[5], Gottfried Weissenböck[4] and Jörg-Peter Schnitzler[2,6]

[1] *GSF-Forschungszentrum für Umwelt und Gesundheit, Institut für Pathologie, Neuherberg, D-85764 Oberschleißheim, Germany*

[2] *Fraunhofer-Institut für Atmosphärische Umweltforschung, Kreuzeckbahnstr. 19, D-82467 Garmisch-Partenkirchen, Germany*

[3] *GSF-Forschungszentrum für Umwelt und Gesundheit, Institut für Biochemische Pflanzenpathologie, Neuherberg, D-85764 Oberschleißheim, Germany*

[4] *Botanisches Institut der Universität Köln, Gyrhofstr. 15, D-50923 Köln, Germany*

[5] *Lehrstuhl für Pharmazeutische Biologie der Universität Würzburg, Mittlerer Dallenbergweg 64, D-97082 Würzburg, Germany*

Received 23 October 1997; Accepted 25 February 1998

Abstract

Phenolic compounds are involved in many interactions of plants with their biotic and abiotic environment. These substances accumulate in different plant tissues and cells during ontogenesis and under the influence of various environmental stimuli, respectively. Studies on the tissue localization of phenolic compounds provide a fundamental prerequisite for understanding the ecological functions of these compounds. The present work shows the localization of various phenolics in cell walls, vacuoles, and associated with cell nuclei, in leaves of a monocotyledonous and a dicotyledonous plant, in a gymnosperm as well as in rhizomes of a horsetail by confocal laser scanning microscopy (CLSM). Using fresh plant material, it compares in detail the tissue localization of autofluorescent styrylpyrones and hydroxycinnamic acids and the visualization of epidermal flavonoid compounds using shift reagents like ammonia, and fluorescence-inducing reagents like Naturstoffreagenz A (diphenylboric acid 2-aminoethyl ester). The comparison of microscopic data obtained from different plant species shows the advantages and limitations of confocal laser scanning microscopy in ecological biochemistry of phenolic plant metabolites.

Key words: Phenolic compounds, histochemistry, confocal laser scanning microscopy, UV-screening pigments, *Picea abies* (L.) Karst., *Vicia faba* L., *Secale cereale* L., *Equisetum arvense* L.

Introduction

Phenolic compounds play a major role in the interaction of plants with their environment (Harborne, 1993). They may attract insects, function as signals between plants (allelopathy), as signals between plants and symbiotic (N_2-fixing bacteria) or pathogenic organisms (phytopathology), and they may protect plants against biotic (e.g. microbial pests, herbivores) or abiotic stresses (e.g. air pollution, heavy metal ions, UV-B radiation). For a basic understanding of ecological functions of phenolic compounds it is essential to know the chemical structure of the compounds of interest, their biosynthetic pathways and its regulation, as well as their tissue localization. Several studies have indicated a high degree of compartmentation of phenylpropanoid and flavonoid compounds and the enzymes involved in their biosynthesis (Knogge and Weissenböck, 1986; Schmelzer *et al*., 1988; Haussühl *et al*., 1996). Phenylpropanoid and flavonoid compounds usually accumulate in the central vacuoles of guard cells and epidermal cells as well as subepidermal cells of leaves (Moskowitz and Hrazdina, 1981; Weissenböck *et al*.,

[6] To whom correspondence should be addressed. Fax: +49 8821 73573. E-mail: schnitzler@ifu.fhg.de

1986; Schnabl *et al*., 1986, 1989) and shoots (Ozimina, 1979). Furthermore, some compounds were found to be covalently linked to plant cell walls (Strack *et al*., 1988; Schnitzler *et al*., 1996), others occur in waxes (Schmutz *et al*., 1994) or on the external surfaces of plant organs (Cuadra and Harborne, 1996). Methods used in localization studies include light microscopy, fluorescence and electron microscopy (Harris and Hartley, 1976; Charest *et al*., 1986), physical (Hrazdina *et al*., 1982; Knogge and Weissenböck, 1986) or enzymatic (Schnitzler *et al*., 1996) tissue preparation before chromatographic analysis or isolation of organelles for enzymatic studies (Hrazdina, 1992) or protoplasts for preparation of vacuoles (Hopp and Seitz, 1987; Anhalt and Weissenböck, 1992).

Direct microscopic observation of phenolic compounds is restricted to anthocyanin-containing tissues, where the target compounds are coloured red, purple or blue. Several classes of phenolic compounds, for example, hydroxycinnamic acids, coumarins, stilbenes, and styrylpyrones (Ibrahim and Barron, 1989; Veit *et al*., 1993; Gorham, 1995), are strongly autofluorescent when irradiated with UV or blue light. Therefore, fluorescence microscopy is a powerful tool for studying tissue localization of these metabolites. To investigate non-coloured and non-fluorescent phenolic compounds, other techniques such as immunocytochemical detection using specific antibodies (Ibrahim, 1992; Grandmaison and Ibrahim, 1996), histochemical staining with chromogenic reagents (e.g. lignin with phloroglucinol/HCl, proanthocyanins with dimethylamino-cinnamaldehyde (Treutter, 1989)) or induction of secondary fluorescence (e.g. flavonoid-staining with Naturstoffreagenz A (Vogt *et al*., 1994; Schnitzler *et al*., 1996; Reinold and Hahlbrock, 1997)) have also been applied.

Recent developments in microscopic techniques, such as confocal laser scanning microscopy (CLSM), provide the opportunity to study tissue localization of phenolic compounds more precisely than by conventional fluorescence microscopy. CLSM aids in the identification of chemical components using their specific fluorescence characteristics, on the basis of their absorbance and emission behaviour. The technique is particularly advantageous for 3-D imaging of thick samples (e.g. 'free hand'-sections) based on the possibility of optical sectioning (Sheppard, 1993; Fricker *et al*., 1997). It also allows the selection of sections (oriented in arbitrary directions), by x-z imaging sections perpendicular to the system plane, as demonstrated in the present paper. The technique also enables the differentiation between various phenolic compounds, selecting spectral excitation and emission bands by minimizing overlapping of the spectral detection channels within the same plant tissue.

The present paper summarizes the results of our comparative CLSM study using leaves of representatives of monocotyledonous, dicotyledonous, and gymnosperm plants as well as of laser-induced fluorescence microscopy from rhizomes of horsetail.

Materials and methods

Chemicals

Equisetumpyrone and dicaffeoyl-*meso*-tartaric acid were isolated from *Equisetum arvense* L. gametophytes. Buffer reagents and other chemicals were obtained commercially and were of analytical grade.

Plant material, growth and irradiation conditions

Four-year-old Norway spruce trees (*Picea abies* (L.) Karst.) were purchased from the Staatliche Samenklenge Laufen (No. 4303, origin Schongau, Bavaria, Germany). Current-year needles (1996) at different developmental stages were used for the experiments. Spores of *E. arvense* L. were collected from plants of the botanical garden in Würzburg, and gametophytes were derived from single spore cultures which were repeatedly subcultured for 6 weeks in a growth chamber on Murashige and Skoog's medium (0.8% agarose (w/v)) under photosynthetic photon flux densities (*PPFD*) between 20 to 50 μmol m^{-2} s^{-1}. Rye seedlings (*Secale cereale* L.) were grown on a watered peat/soil mixture under a 13/11 h light–dark regime at 20/10 °C day/night temperature and 50/80% relative humidity (RH) in a phytotron at a maximum of 750 μmol m^{-2} s^{-1} *PPFD*. Primary leaves of 5-d-old seedlings were harvested for CLSM analysis. *Vicia faba* L. cv. Con Amore plants were grown from seeds in standard soil (Fruhstorfer, type T, Archut, Lauterbach, Germany) in a sun simulator (Seckmeyer and Payer, 1993) at 18/13 °C day/night temperature, 70/90% RH and a daily 12 h light period with a maximum *PPFD* of 800 μmol m^{-2} s^{-1}. For CLSM analysis secondary leaves were used.

Confocal laser scanning microscopy (CLSM)

The basic principle of CLSM is illustrated in Fig. 1. The specimens were illuminated through the imaging lens with the critical illumination scheme (Michel, 1962). A diffraction limited light spot was produced within the sample with a laser light source (Sheppard, 1993). Re-emitted light, i.e. the stokes shifted fluorescence, was imaged by the microscope lens, deflected by a beam splitter and detected by a photomultiplier. Thus, the image of one point of the sample was obtained. To generate a two-dimensional image, the focused spot was moved across the sample by a x-y light deflector. Thus the image was detected sequentially, point by point and line by line. So far, the images from laser scanning and conventional epifluorescence microscopy are quite similar. The optical sectioning was achieved by application of a confocal filter. This is realized by a small pinhole in the image plane in front of the detector. The experimental object was adjusted so, that the light emitted from an illumination spot was focused exactly into the pinhole, and thus could pass without attenuation to the detector. The light originating from layers above or below the focused plane was focused before or behind the pinhole, and was thus weakened considerably. Elimination of unfocused light depends on the numerical aperture of the microscope lens and the size of the pinhole. Under optimal conditions the axial (in depth) resolution is about three times lower than the lateral resolution given by wavelength [nm] numerical $aperture^{-1}$ (Wallén *et al*., 1992). The CLSM analysis was performed with a Zeiss Axiovert 100 microscope (Zeiss, Oberkochen, Germany). Throughout this work a single line excitation and multiple channel emission

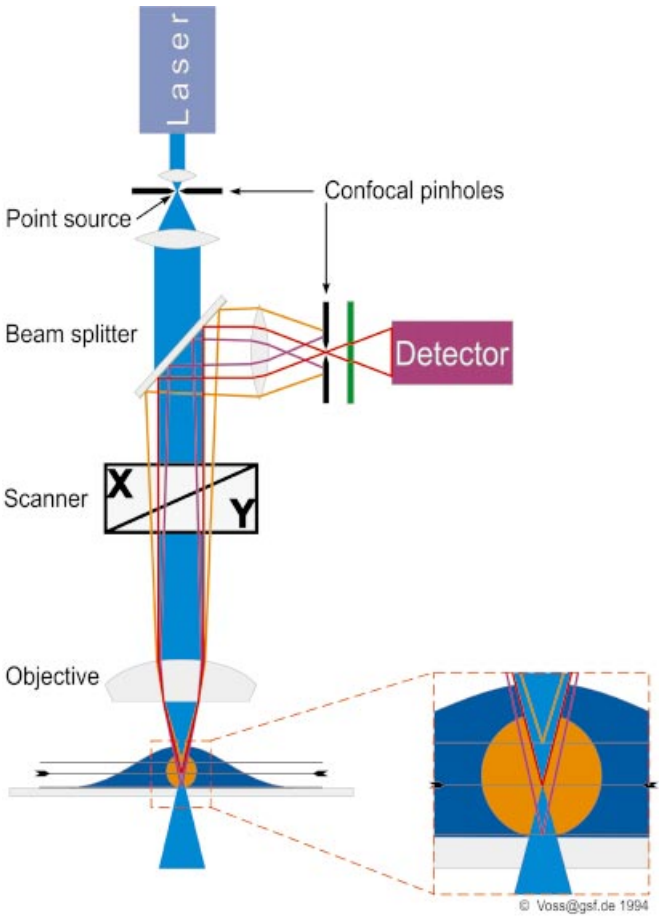

Fig. 1. Schematic diagram of a confocal laser scanning microscope. Light which does not originate from the focal plane (- - - or —) is defocused at the confocal aperture and thus detected only weakly.

technique was used. For visualization of multispectral image data, the different channels are generally associated with a colour value on the display system. When there are no more than three fluorescence channels, it is most convenient to assign the primary display colours ('pseudo-colours') red, green and blue (RGB-colour mode). For example, when a UV excitation is used (laser line at 364 nm), the fluorescence channel is given by the band pass filter (BP) 400–430 nm (blue), BP 515–565 nm (green) and longpass filter (LP) >590 nm (red). All fluorescence channels are measured simultaneously. The visual colour impression from the screen does not necessarily correspond with visual impressions obtained with a multiline filter set or an LP filter. Furthermore, the ratios of signals from different channels differed from real time viewing due to filter transmittance, exposure time and detector sensitivity.

Besides the CLSM pictures of *Vicia*, *Secale*, and *Picea* presented, laser-induced fluorescence images from *Equisetum* rhizomes were taken with a cooled, integrating CCD camera (Photometrics AT 200) mounted on a Zeiss Axiovert 100 microscope with an HBO 50 excitation lamp (Zeiss, Oberkochen, Germany).

Samples of *Vicia*, *Secale*, and *Picea* (treated with ammonia, with NA, or untreated, respectively) were monitored under identical conditions and with identical buffer solutions. Single x-y images as well as series of x-z images were taken from all samples.

Fluorescence emission spectra of selected compounds

Autofluorescence of dicaffeoyl-*meso*-tartaric acid (25 μM in MeOH) and equisetumpyrone (37 μM in MeOH), respectively, was measured with a fluorimeter (Perkin Elmer LS 50 Luminescence Fluorimeter, Überlingen, Germany) at the excitation wavelengths of 364 and 488 nm as used in CLSM and laser-induced conventional fluorescence microscopy. The emission spectra were monitored from 385–660 nm and 420–600 nm, respectively.

Sample preparation for histochemical analysis

Fresh leaves of *V. faba* L., *S. cereale* L., and *P. abies* (L.) Karst., were cut with a razor blade and cross, longitudinal, and paradermal sections of the leaves were incubated on microscopic slides in a droplet (100 μl) of sample buffer (100 mM KP_i pH 6.8, 1% NaCl (w/v)) under a coverslip, and autofluorescence of the samples was studied by CLSM. Sections of living rhizomes of *E. arvense* were incubated on microscopic slides in a droplet (100 μl) of an aqueous solution of 50% PEG 400 (w/v) containing 1 M NaCl. Cross-sections of *Equisetum* were additionally washed with H_2O prior to conventional microscopy and CLSM.

In situ *treatment with aqueous ammonia*

After monitoring the autofluorescence of leaf sections of *Vicia*, *Secale*, and *Picea*, a droplet of freshly prepared 0.5% (w/v) ammonia in sample buffer was added and transferred under the coverglass using filter paper. Fluorescence of the samples was studied at the identical position in the leaf sections using identical microscopic conditions as in the buffer control.

In situ *staining with Naturstoffreagenz A (NA)*

As described for ammonia treatment, the autofluorescence of leaf sections of *Vicia*, *Secale*, and *Picea* was monitored. Afterwards, a droplet of 0.1% (w/v) NA in sample buffer (same NA-solution for all samples, and prepared immediately before use from a stock solution of 2.5% (w/v) NA in EtOH) was added and transferred under the coverglass as described above. Samples were incubated for 5 min, and the NA solution was then removed by excessive transfering of buffer under the coverslip. Fluorescence of NA-stained phenolic compounds was studied at the same position of the sections using the same microscopic conditions as in the buffer control.

Results and discussion

Autofluorescence of soluble and cell wall-bound phenolic metabolites

In recent years, various flavonoids, caffeic acid esters, and styrylpyrones (Fig. 2) have been isolated from different organs of *Equisetum* species (Veit *et al.*, 1995). The accumulation of these compounds is tissue specific, depending on the stage of organ development and induction stimuli. Equisetumpyrone and dicaffeoyl-*meso*-tartaric acid accumulate as the major phenolic constituents in gametophytes and rhizomes of *E. arvense* L. No flavonoids were detected in these organs (Veit *et al.*, 1995; Beckert *et al.*, 1997). Equisetumpyrone and dicaffeoyl-*meso*-tartaric acid are strongly autofluorescent when excited at appropriate wavelengths. Figure 3 shows the

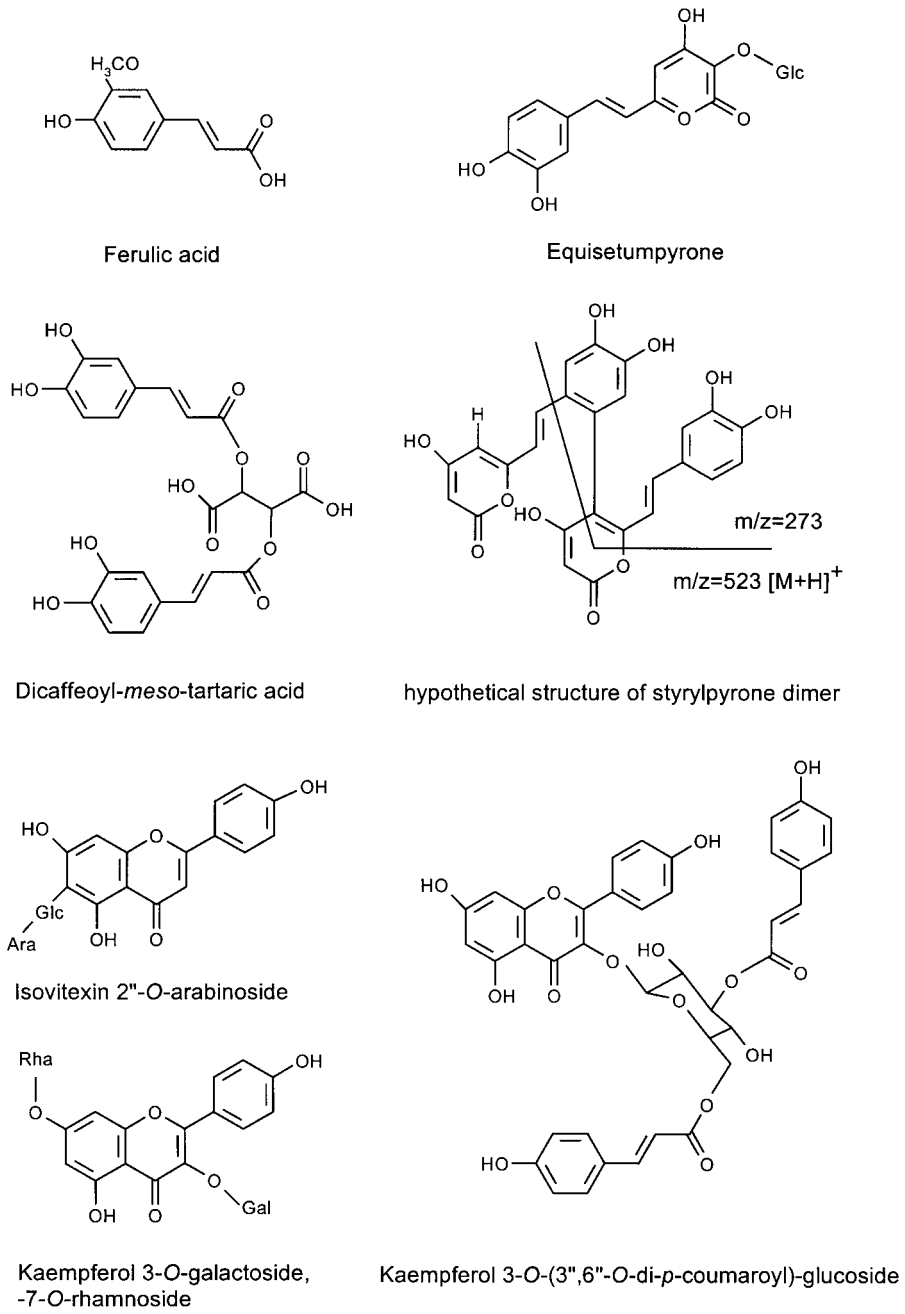

Fig. 2. Chemical structures of major phenolic compounds from the plant species studied. *Equisetum*: equisetumpyrone, dicaffeoyl-*meso*-tartaric acid, hypothetical structure of a styrylpyrone dimer (as indicated from the mass spectrometric fragments indicated) released from cell walls of *Equisetum arvense* rhizomes with dioxane/HCl; *Vicia*: kaempferol 3-*O*-galactoside, 7-*O*-rhamnoside; *Secale*: Isovitexin 2″-*O*-arabinoside, ferulic acid; *Picea*: kaempferol 3-*O*-(3″,6″-*O*-di-*p*-coumaroyl)-glucoside.

fluorescence spectra of the respective pure compounds excited at the UV (364 nm) and blue (488 nm) laser lines, which were also used in the CLSM experiments. The signals of the two metabolites excited at 364 nm could be separated based on their characteristic emission spectra. The emission spectrum of dicaffeoyl-*meso*-tartaric acid reached a maximum at 440 nm, whereas the emission spectrum of equisetumpyrone peaked at approximately 490 nm. Excitation at 488 nm resulted only in autofluorescence of equisetumpyrone with an emission maximum at 555 nm, whereas no fluorescence was observed for dicaffeoyl-*meso*-tartaric acid under these conditions. The spectra were recorded in methanol, because cell free aqueous solutions of these compounds had very low fluorescence intensity. This is in contrast to the situation *in situ*, presumably due to intermolecular interaction or molecular complexing similar to that described for anthocyanins (Brouillard and Dangles, 1986). Using the spec-

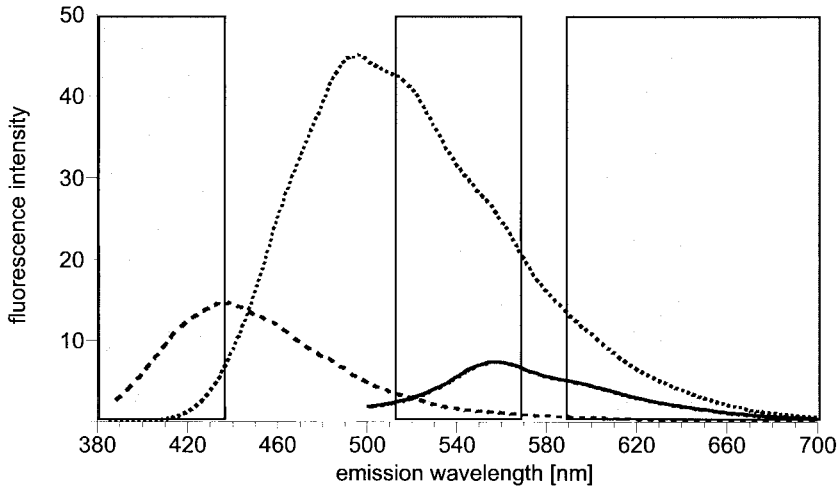

Fig. 3. Emission spectra of dicaffeoyl-*meso*-tartaric acid (25 μM in MeOH), excited at 364 nm (—-) and equisetumpyrone (37 μM in MeOH), excited at 364 nm (.....) and 488 nm (- - -). Grey areas represent the bandwidth of the filters used in fluorescence microscopy.

troscopic information, the fluorescence of both compounds could be differentiated in the plant tissue by appropriate choice of excitation wavelength and emission filters as is demonstrated in Fig. 4.

Figure 4 shows the autofluorescence of *Equisetum* rhizomes (Fig. 4a–d), of a primary leaf (Fig. 4e), and a Norway spruce needle (Fig. 4f), furthermore the figure shows a comparison of the fluorescence signals obtained by conventional microscopy and CLSM. When cross-sections of *Equisetum* rhizomes (Fig. 4a) were excited at 364 nm, the fluorescence signal measured in the blue pseudo-colour channel (band pass 400–430 nm) primarily represented fluorescence of caffeic acid esters, for example, dicaffeoyl-*meso*-tartaric acid, with a contribution from styrylpyrones, for example, equisetumpyrone. Fluorescence detected in the green pseudo-colour channel (515–565 nm) (Fig. 4b), on the other hand, represented the emission of styrylpyrones with little interference from caffeic acid esters. Fluorescence, following excitation at 488 nm originates only from styrylpyrones (Fig. 4c). Although the caffeic acid esters accumulate in equal amounts in the rhizome tissues (Beckert *et al.*, 1997), the cross-sections indicated a concentration gradient of styrylpyrones with lowest concentrations in the central cylinder and increasing concentrations towards the outer cortex (Fig. 4b, c). However, fluorescence in the central cylinder and the inner cortex of the rhizomes sections appeared to be associated exclusively with the cell walls; it originates predominantly from soluble compounds which were released from cells during sectioning. This has been shown by tissue compartmentation analysis of soluble and cell wall bound compounds in the central cylinder, inner cortex and outer cortex of *Equisetum* rhizomes (M Veit, unpublished results). Soluble styrylpyrones could be detected in all tissues. Only in the outer cortex additional compounds bound to the cell walls were detected. They were released from cell wall preparations with dioxane/HCl and were preliminary identified as styrylpyrone dimers by LC-MS experiments (for a proposed structure see Fig. 2; M Veit, unpublished results). The accumulation of the cell wall bound compounds is visualized in Fig. 4c by the colour shift of the fluorescent signal to longer wavelength in this area.

Due to destruction of tissue and cells during sectioning as mentioned above, no information on the subcellular compartmentation of these phenolic compounds was obtained from the cross-sections. Longitudinal sectioning, however, left cells intact to a large extent and subcellular compartmentation could be visualized. Intact cells with intact protoplasts are readily visible upon plasmolysis after adding 1% NaCl (Fig. 4d). The blue pseudo-colours originating from autofluorescent caffeic acid esters and styrylpyrones predominate in the protoplasts, while the green pseudo-colour is visible from the cell walls thus indicating the exclusive presence of styrylpyrones in this compartment.

'Free hand'-sections, in particular, are usually thicker than the depth of focus obtained by lenses with high numerical apertures as used throughout this study. Conventional fluorescent as well as non-confocal laser-induced images were therefore superimposed by a diffuse brightness from layers out of focus (Fig. 4a, b, d). A substantial increase in image quality was obtained using the confocal imaging technique (e.g. compare Fig. 4c, e, f). It allowed optical sectioning through thick samples without requiring thin, mechanical cutting. Figure 4 shows such optical sections with an approximate thickness of 1.2 μm from a primary leaf of rye (Fig. 4e) and a cross-section of a Norway spruce needle (Fig. 4f). In both images, red fluorescence is attributed to chlorophyll in the chloroplasts, as can be seen in detail in Fig. 4e. Previous work on rye primary leaves (Schmitz *et al.*,

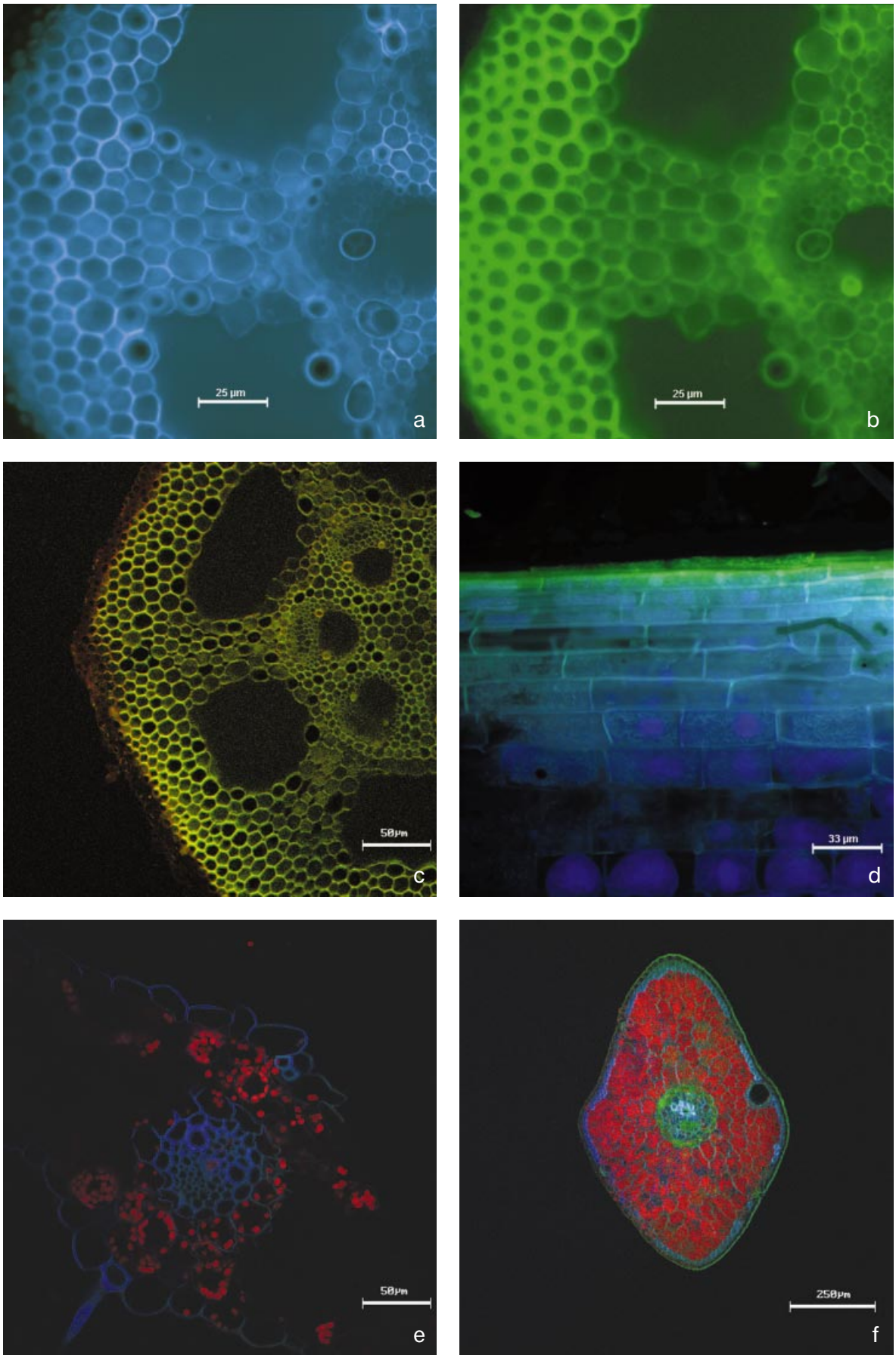

1996) demonstrated that the blue autofluorescence, as seen in the outer periclinal and anticlinal epidermal cell walls and in the phloem walls of the vascular bundle (Fig. 4e), resulted from ferulic acid bound to the cell wall, while the fluorescence in the xylem vessel walls was attributed to lignin. In Norway spruce needles (Fig. 4f) strong blue autofluorescence was observed in cell walls of subepidermal cells, in particular, in cells surrounding the resin ducts and within the cell walls of the xylem. This pattern corresponds to the distribution of lignin as shown by histochemical studies with phloroglucinol/HCl-staining (Polle *et al*., 1994). In addition, a pseudo-green autofluorescence especially in the cuticle, the endodermis, and the cell walls of the phloem of the needle was observed which could not be attributed to specific phenolic compounds. When excited by UV laser light (337 nm), similar pseudo-green autofluorescence in cuticles of wheat and soybean has been described by Stober and Lichtenthaler (1993), but it has not been assigned to any known phenolic structure(s).

Fluorescence induction by alkalization with ammonia

Figure 5 demonstrates the effect of alkalization of intact plant tissue by adding 0.5% ammonia to the sample buffer. Identical cells of cross-sections of broad bean (Fig. 5a, b) and paradermal sections of rye leaves (Fig. 5c, d) were excited at 364 nm. Fluorescence was studied prior to (Fig. 5a, c) and after (Fig. 5b, d) ammonia treatment.

Prior to alkalization in broad bean cross-sections only red-imaged chorophyll fluorescence in the mesophyll, and blue fluorescence attributed to phenolic compounds in some mesophyll cells, and in the cuticle or in the outer periclinal cell wall of the epidermis were detected (Fig. 5a). Incubation of broad bean leaves with ammonia and excitation at 364 nm resulted in strong pseudo-green fluorescence localized in the epidermal cells of the broad bean leaf, and weak pseudo-green fluorescence in subepidermal cells (Fig. 5b). Structural analysis of flavonoid compounds and characterization of fluorescence behaviour of the isolated compounds *in vitro* and *in vivo* (Schnabl *et al*., 1986) indicated that the green fluorescence in broad bean epidermal cells originates from kaempferol glycosides (Vierstra *et al*., 1982; Weissenböck *et al*., 1984; Schnabl *et al*., 1986; Thomás-Lorente *et al*., 1989), which are known to be strongly fluorescent only in alkaline solutions.

Earlier studies on tissue localization have shown that mesophyll cells of rye leaves accumulate two luteolin glucuronides, whereas in epidermal cells, two isovitexin derivatives, isovitexin 2″-*O*-arabinoside (Fig. 2) and isovitexin 2″-*O*-galactoside are present (Schulz and Weissenböck, 1986). Furthermore, primary leaves of rye contain high concentrations of soluble hydroxycinnamic acid esters (Strack *et al*., 1987), which have been exclusively detected in epidermal cells (Schulz and Weissenböck, 1986).

As outlined above (see also Fig. 4e), ferulic acid is the major alkali-extractable phenolic compound in the cell walls of the leaf vascular bundle with the exception of cell walls of the xylem (Schmitz *et al*., 1996). Ferulic acid also occurs in epidermal cell walls of rye primary leaves (Figs 5c, 6d). In the section displayed, pseudo-blue fluorescence resulting from phenols bound to the cell wall were detectable in anticlinal cell walls and even more prominently in guard cell walls. Incubation with ammonia (Fig. 5d) led to a shift of the blue fluorescence to longer wavelengths. This indicates that the fluorescence is related to cell wall-bound ferulic acid derivatives (Harris and Hartley, 1976; Schmitz *et al*., 1996). The strongest fluorescence occurred in the walls of the guard cells and the basal cells of the trichomes. No fluorescence of the flavone glycosides was detectable within the cells of rye epidermal cells. The fluorescence observed in the left part of the image (Fig. 5d) results from the phenols located in the cuticle and outer periclinal cell walls. In this area the CLSM section is located within the outer periclinal cell wall and cuticle while in the middle and right part of the image the optical section hits the lumen of both epidermal and mesophyll cells.

Coniferous leaves such as Norway spruce needles are rich in soluble and wall-bound phenolic compounds of different classes, such as hydroxycinnamic acid derivatives, lignans, coumarins, stilbenes and flavonoids (Strack *et al*., 1988; Heilemann, 1990). Recent work using enzymatically prepared epidermal layers of Scots pine needles, Schnitzler *et al*. (1996) demonstrated the almost exclusive epidermal localization of wall-bound hydroxycinnamic acids and kaempferol 3-*O*-glucoside as well as soluble diacylated flavonol glucosides, e.g. kaempferol 3-*O*-(3″,6″-*O*-di-*p*-coumaroyl)-glucoside and related derivatives (Fig. 2). This diacylated flavonoid represents the main metabolite of this structural class in Norway spruce epidermal cells (R Fischbach and JP Schnitzler, unpublished results). Blue excited (488 nm) strong pseudo-yellow fluorescence in cell walls and protoplasts of the epidermal cells was revealed in paradermal (Fig. 5e) and

Fig. 4. Autofluorescence of (a–d) *Equisetum* rhizome, (e) rye primary leaf, and (f) Norway spruce needle. Cross (a–c) and longitudinal (d) sections of *Equisetum* rhizomes were embedded in aqueous 50% PEG 400 (w/v) containing 1 M NaCl, and pictures were taken with CCD camera (a, b, d) or in CLSM technique (c). (a) B-colour mode laser-induced (364 nm); (b) G-colour mode laser-induced (488 nm); (c) RG-colour mode laser-induced (488 nm); (d) GB-colour mode UV laser-excited (364 nm). (e) RGB-colour mode UV laser-excited (364 nm) autofluorescence of primary leaves of rye in buffer (100 mM KPi pH 6.8, 1% NaCl (w/v)). (f) RG-colour mode blue laser-excited (488 nm) autofluorescence of needles of Norway spruce in buffer (100 mM KPi pH 6.8, 1% NaCl (w/v)).

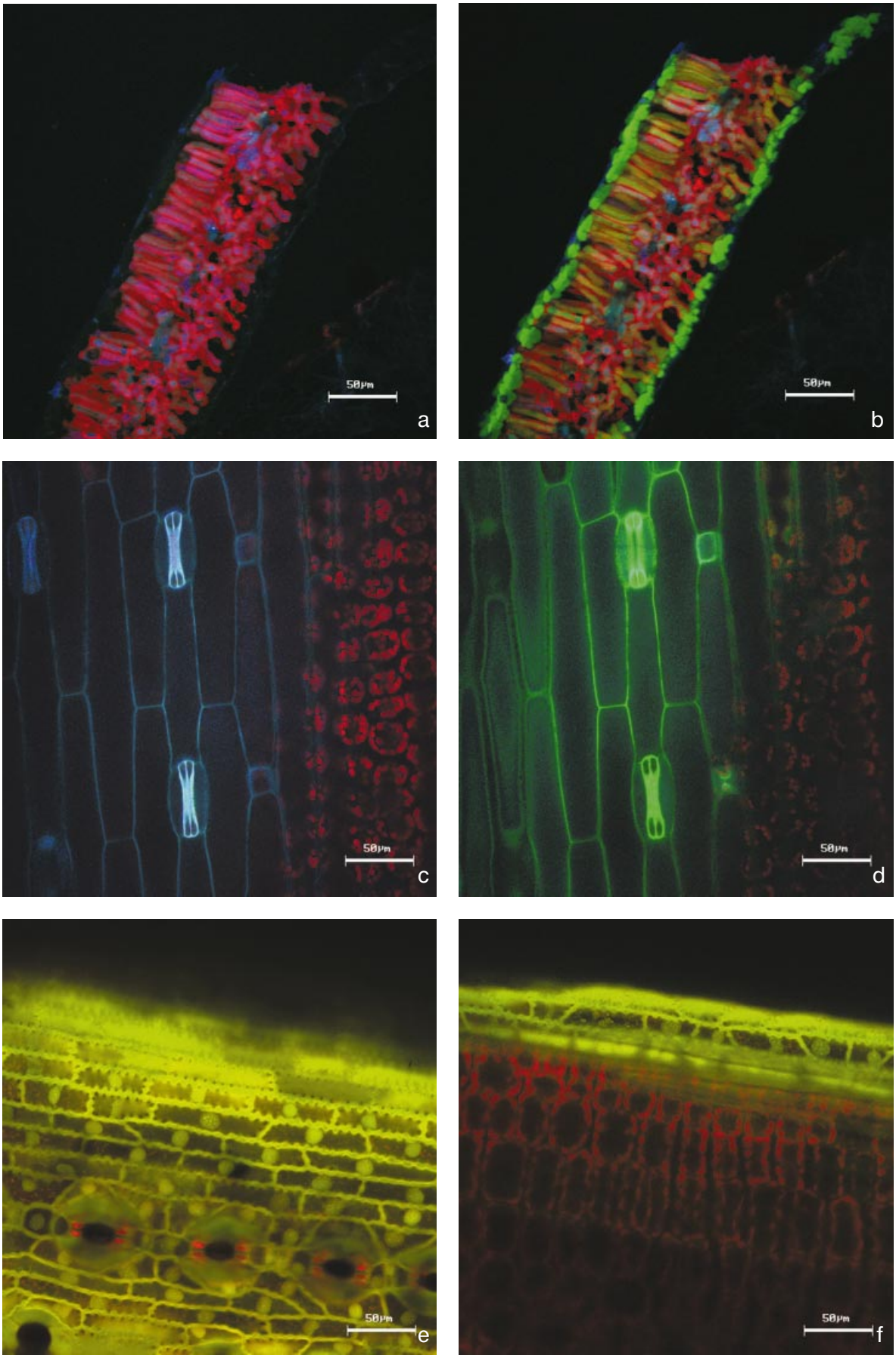

longitudinal sections (Fig. 5f) of needles after ammonia treatment. The optical plane of the CLSM section in Fig. 5e cuts all parts of the uneven epidermal surface of the spruce needle. At the top of the figure the fluorescence of the cuticle and outer periclinal walls is seen. Progressing towards the interior of the needle, the lumen of epidermal and stomatal cells showed a distinct fluorescence associated with the nucleus and the cytoplasma of epidermal cells, while no fluorescent signal was obtained in the vacuole. In addition, the ammonia-induced fluorescent signals were restricted to the epidermal needle tissue (Fig. 5f). In broad bean (Fig. 5b), treatment with the same buffer stimulated vacuolar fluorescence, as has been described for many flavonoid compounds (Vierstra *et al*., 1982; Hrazdina *et al*., 1982; Schnabl *et al*., 1986). This indicates that the observed pattern in spruce is not an artefact, and similar results were obtained with NA-staining (see below and Fig. 6).

Fluorescence induction with Naturstoffreagenz A

Naturstoffreagenz A is a well-known reagent used in paper and thin layer chromatography to visualize flavonoid compounds where inducing secondary fluorescence is induced (Markham, 1982). It has earlier been shown that the reagent can also be applied in histochemistry for the detection of flavonoid compounds (Schnitzler *et al*., 1996). Figure 6a shows the NA-staining of flavonol glucosides (for structures see Fig. 2) in epidermal layers of broad bean leaves. Excitation with a UV laser beam of 364 nm induced strong pseudo-green fluorescence in epidermal cells, which is attributed to the flavonol glycosides present in the vacuole (see also Fig. 6b). Since the position of the optical section in Fig. 6a is below the cuticle surface and passes several times the uneven outer periclinal cell wall of the epidermis, the pseudo-blue fluorescence originating from the cuticle is also visible.

Flavonoid staining with NA in Fig. 6 demonstrates one of the most important advantages of CLSM compared to conventional fluorescence microscopy. The ability to scan in the x-z direction perpendicular to the system axis allows one to study the distribution of phenolic compounds in a three-dimensional manner (Fig. 6b, c, g, h). Using this approach spatial information was obtained from the fluorescence signal. The locations of x-z-scans are marked by arrows within the respective x-y figures (Fig. 6b, c, g, h). Figure 6b shows the situation in broad bean. Since the x-z scans of the paradermal leaf section passes the middle of the vacuoles, the homogeneously distributed NA-induced secondary fluorescence, visible within the lumen of the plasmolysed cells, demonstrates the presence of flavonol glucosides within the cell vacuole. In addition, the attenuation of the laser beam within the epidermal layer can be recognized. The fluorescence attributed to flavonoids declined in the epidermal cells with distance to the leaf surface. Chlorophyll fluorescence from the underlying mesophyll cells was only detected in the gaps between the plasmolysed epidermal cells. The data from broad bean leaves stained with NA clearly confirm the results obtained by ammonia enhancement of fluorescence depicted in Fig. 5b.

Figures 6d and 6e show the same area of rye epidermal cells prior to and after staining with NA. In Fig. 6d, only chlorophyll and pseudo-blue autofluorescence of cell wall-bound ferulic acid derivatives are visible, especially in stomatal cell walls. Addition of NA revealed pseudo-green fluorescence signals within the cell lumen which were attributed to epidermal isovitexin derivates (Schulz and Weissenböck, 1986). Comparable to broad bean leaves, the x-z-scan of the rye sample (Fig. 6c) shows the homogeneous distribution of flavonoid-related fluorescence within the epidermal cells as well as the attenuation of induced fluorescence depending on the penetration depth of the laser beam. Since the buffer contains 1% NaCl the epidermal cells have undergone plasmolysis and the NA-induced fluorescence of the flavones can be unequivocally localized within the vacuole.

In spruce, NA-stained fluorescence (excitation at 488 nm) of flavonoids was exclusively restricted to the epidermal cell layer of the needle (Fig. 6f, g, h). Strong fluorescence was also visible in the cell wall of the epidermal layer of spruce needles, indicating the occurrence of wall-bound flavonol derivatives. The major flavonoid compound in spruce and pine cell walls has earlier been shown to be kaempferol 3-*O*-glucoside (Strack *et al*., 1988; Schnitzler *et al*., 1996).

Coniferous needles are known for their ability to absorb short-wavelength radiation effectively (DeLucia *et al*., 1992; Day *et al*., 1994), while in herbaceous leaves higher amounts of UV-B radiation can penetrate the mesophyll (Reuber *et al*., 1996). The ability of CLSM to scan in the x-z dimension of the sample clearly demonstrates that (Fig. 6a, e, f). Comparison of x-z scans from epidermal layers of all three species demonstrated (Fig. 6b, c, g) that in broad bean and rye leaves, radiation of 364 nm stimulated fluorescence within the vacuole, whereas, in spruce, virtually all 364 nm radiation of the laser was absorbed by the first micrometers of the outer cell wall and the cuticle. Excitation of NA-induced fluorescence

Fig. 5. CLSM images of ammonia-induced fluorescence in broad bean (a, b), rye (c, d) and Norway spruce (e, f). (a, b) RGB-colour mode UV laser-excited (364 nm) fluorescence of an identical broad bean leaf cross-section prior (a) and after (b) incubation in ammonia (0.5% in sample buffer). (c, d) RGB-colour mode UV laser-excited (364 nm) fluorescence of an identical rye leaf paradermal section prior (c), and after incubation in ammonia (0.5% in sample buffer). (e) RG-colour mode blue laser-excited (488 nm) fluorescence of Norway spruce paradermal section incubated in ammonia (0.5% in sample buffer). (f) RG-colour mode blue laser-excited (488 nm) fluorescence of Norway spruce longitudinal section incubated in ammonia (0.5% in sample buffer).

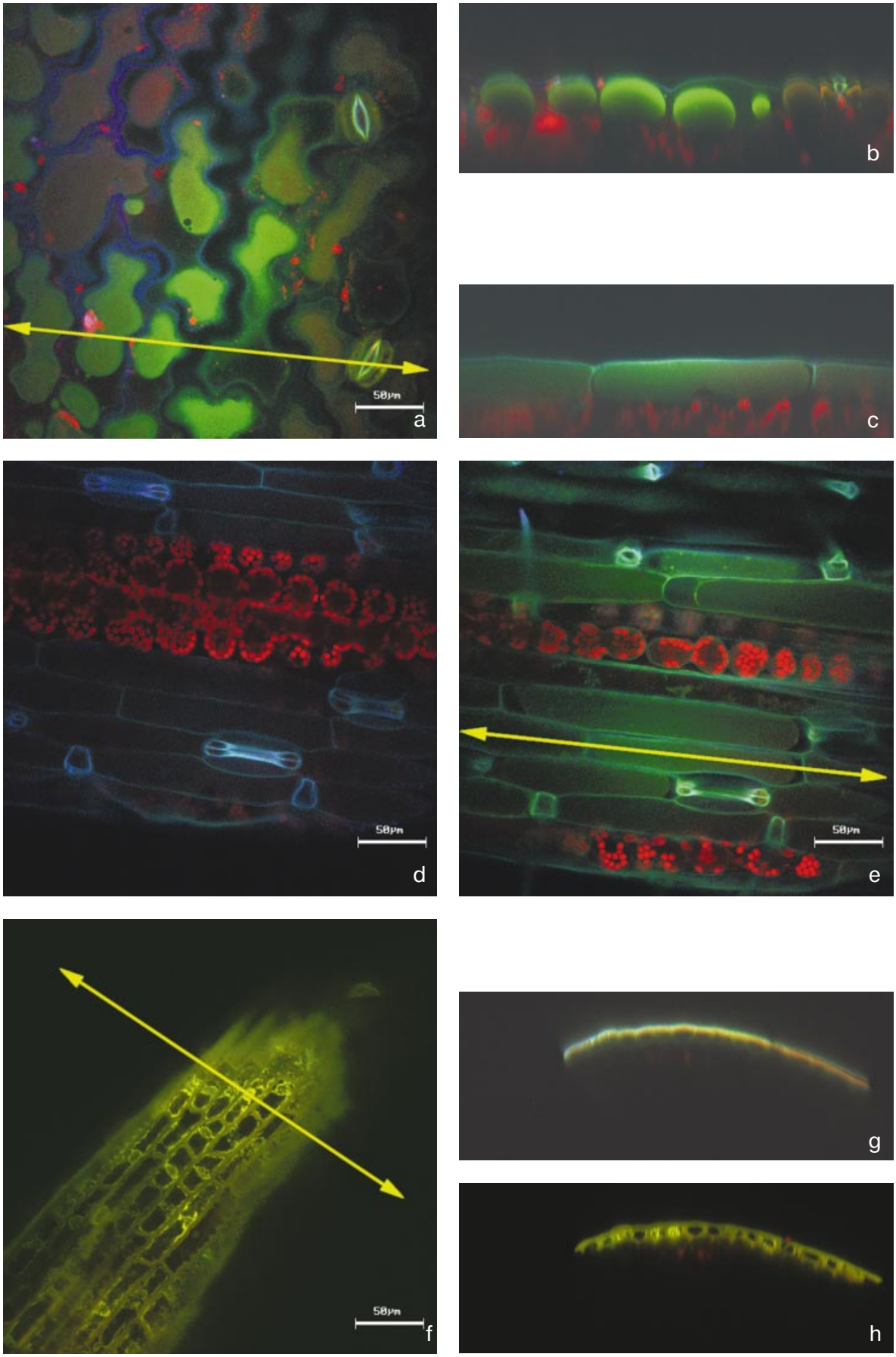

of the diacylated flavonol glucosides in the epidermal cells of the spruce needle only occurred at the excitation wavelength of the blue laser beam (488 nm). Comparison of the x-z scan images of broad bean, rye and spruce leaves (Fig. 6b, c, g), confirmed the different UV-screening effectiveness of these leaves which is correlated with the live plant form as measured by fibre-optical microprobe techniques (Day, 1993; Day *et al*., 1994). While epidermal attenuation of UV-radiation in annual herbs (broad bean and rye) is mostly due to vacuolar pigments, incident UV-radiation was strongly attenuated also by cell wall-bound phenols such as kaempferol 3-*O*-glucoside in the evergreen coniferous needles of Norway spruce.

Different subcellular distribution patterns of flavonoid metabolites are observed for leaves of annual and evergreen plants. In broad bean and rye, fluorescent NA-stained flavonoid complexes are present in the vacuole, while in the epidermal cells of the spruce needle, similar to the situation after ammonia treatment (Fig. 5e, f), strong fluorescence signals are only detected in the cytoplasm and associated with the cell nucleus, accompanied by a complete absence of fluorescence within the vacuole. The occurrence of flavonoids in the nucleus region of spruce epidermal cells, as observed microscopically with both types of staining, as well as the observed absence of vacuole-related fluorescence has to be confirmed by further experiments with other staining reagents or other techniques.

Evidence for nucleus-related flavonoids came from recent work with *Arabidopsis* (Sheahan, 1996), and *Flaveria* (Grandmaison and Ibrahim, 1996). In *Flaveria* the association of flavonol sulphate esters with the nuclei and the cytoplasma as well as the specific binding of quercetin 3-sulphate to nuclear proteins have been demonstrated. The occurrence of nucleus-related flavonoids give rise to many open questions concerning, for example, their effectiveness in protecting DNA from UV-B damage, and their possible function as antioxidants under oxidative stress, especially since the flavonol glycosides of Norway spruce are diacylated with *p*-coumaric and ferulic acids, well known as radical scavengers (Bors *et al*., 1990; Rice-Evans *et al*., 1997).

Conclusions

In the present paper autofluorescence and secondary fluorescence induced by ammonia- and NA-treatment were applied to several different plant species and compared to characterize tissue localization of different phenolic compounds including cell walls, vacuoles, and possibly cell nuclei. Main emphasis was put on the investigation of autofluorescent compounds after excitation with UV, and blue laser, and the visualization of epidermal UV-B screening pigments.

The ability of CLSM to create three-dimensional images is an important feature for scientists from various areas, ranging from ecology to plant pathology. As demonstrated in the present work, x-z images can be used to demonstrate light attenuation within leaf surfaces. In combination with the fibre-optic microprobe technique (Day *et al*., 1994) CLSM may help to explain the various UV-B screening abilities of different plant species. The same technique may be used to study the three-dimensional distribution of phenolic compounds around infection sites after microbial or herbivore attack or around necrotic spots induced by abiotic factors like ozone. This technique also makes it possible to obtain information about the subcellular localization of phenolic compounds, in particular whether or not the signal is derived from the vacuole or cell wall. Another advantageous property of CLSM is the ability to obtain quantitative information about the fluorescence intensities (Fricker *et al*., 1997). Since the images are measured in form of electronic signals, a whole range of electronic processing techniques can be employed, and images from different treatments can be compared.

Recently, the application of UV laser-induced fluorescence has received considerable attention with respect to remote LIDAR techniques for screening the health status of terrestrial vegetation (Stober and Lichtenthaler, 1993; Subhash *et al*., 1995). Application of CLSM using the same laser lines may now provide basic biochemical information for the interpretation of LIDAR remote data.

Like conventional fluorescence, interpretation of CLSM is hampered by the fact that the chemical nature of fluorescent compounds has to be known. Therefore, conclusive microscopic data can still be obtained when rigorously combined with structural analysis of the phenolic compounds, their extraction and verification in isolated tissue, accompanied by physiological studies on the biosynthetic pathways and the site(s) of accumulation.

Acknowledgements

The authors would like to thank Professor H Rennenberg, University of Freiburg and Dr R Steinbrecher, Fraunhofer-

Fig. 6. CLSM images of Naturstoffreagenz A (NA)-stained fluorescence in broad bean (a, b), rye (c, d, e) and Norway spruce (f, g, h). (a) RGB-colour mode UV laser-excited (364 nm) fluorescence of broad bean leaf paradermal section stained with NA (0.1% (w/v) in sample buffer). (b) x-z scan of the same section displayed in (a). (d, e) RGB-colour mode UV laser-excited (364 nm) fluorescence of rye primary leaf paradermal section prior (d) and after (e) incubation in NA (0.1% (w/v) in sample buffer). (c) x-z scan of the rye primary leaf paradermal section displayed in (e). (f) RG-colour mode blue laser-excited (488 nm) fluorescence of Norway spruce needle paradermal section incubated in NA (0.1% (w/v) in sample buffer). (g) x-z scan of RGB-colour mode UV laser-excited (364 nm) fluorescence of the same section displayed in (f), (h) x-z scan of RG-colour mode blue laser-excited (488 nm) fluorescence of the Norway spruce paradermal section displayed in (f). Arrow lines describe the positions of the x-z scans.

Institut für Atmosphärische Umweltforschung, Garmisch-Partenkirchen, for critical reading of the manuscript, and Pat Hahn for helpful linguistic improvements. We are also grateful to A Voss, GSF-Institut für Pathologie, Neuherberg, for his excellent technical advice in fluorescence spectrophotometry. The work was partly supported by 'BayFORKLIM' (Bayer. Staatsministerium für Unterricht, Kultur, Wissenschaft und Kunst (MV project U9); Bayer. Staatsministerium für Landesentwicklung und Umweltfragen (project U11 (WH) and project U5 (RF and JPS)). The authors SR, RS and GW are grateful for the support by the Deutsche Forschungsgemeinschaft (DFG).

References

Anhalt S, Weissenböck G. 1992. Subcellular localization of luteolin glucuronides and related enzymes in rye mesophyll. *Planta* **187,** 83–8.

Beckert C, Horn C, Schnitzler JP, Lehning A, Heller W, Veit M. 1997. Styrylpyrone biosynthesis in *Equisetum arvense*. *Phytochemisty* **44**, 275–83.

Brouillard R, Dangles O. 1986. Flavonoids and flower colour. In: Harborne JB, ed. *The flavonoids*: *advances in research since* 1986. London: Chapman & Hall, 565–88.

Bors W, Heller W, Michel C, Saran M. 1990. Flavonoids as antioxidants: determination of radical-scavenging efficiencies. *Methods in Enzymology* **186,** 343–55.

Charest PM, Brisson L, Ibrahim RK. 1986. Ultrastructural features of flavonoid accumulation in leaf cells of *Chrysosplenium americanum*. *Protoplasma* **134,** 95–101.

Cuadra P, Harborne JB. 1996. Changes in epicuticular flavonoids and photosynthetic pigments as a plant response to UV-B radiation. *Zeitschrift für Naturforschung* **51c,** 671–80.

Day TA. 1993. Relating UV-B radiation screening effectiveness of foliage to absorbing-compound concentration and anatomical characteristics in a diverse group of plants. *Oecologia* **95,** 542–50.

Day TA, Howells BW, Rice WJ. 1994. Ultraviolet-B absorption and epidermal transmittance spectra in foliage. *Physiologia Plantarum* **92,** 207–18.

DeLucia EH, Day TA, Vogelmann TC. 1992. Ultraviolet-B and visible light penetration into needles of two species of sub alpine conifers during foliar development. *Plant*, *Cell and Environment* **15,** 921–9.

Fricker MD, Chow C-M, Errigton RJ, May M, Mellor J, Meyer AJ, Tlalka M, Vaux DJ, Wood J, White NS. 1997. Quantitative imaging of intact cells and tissues by multi-dimensional confocal fluorescence microscopy. *Experimental Biology Online* **2,** 19, http://link.springer.de.

Gorham J. 1995. *The biochemistry of the stilbenoids*. London: Chapman & Hall.

Grandmaison J, Ibrahim RK. 1996. Evidence for nuclear binding of flavonol sulphate esters in *Flaveria chloraefolia*. *Journal of Plant Physiology* **147,** 653–60.

Harborne J. 1993. *Introduction to ecological biochemistry*. London: Academic Press.

Harris PJ, Hartley RD. 1976. Detection of bound ferulic acid in cell walls of the Gramineae by ultraviolet fluorescence microscopy. *Nature* **259,** 508–10.

Haussühl K, Rohde W, Weissenböck G. 1996. Expression of chalcone synthase genes in coleoptiles and primary leaves of *Secale cereale* L. after induction by UV radiation: evidence for a UV-protective role for the coleoptile. *Botanica Acta* **109,** 229–38.

Heilemann J. 1990. Untersuchungen zur Struktur und zum Stoffwechsel phenolischer Sekundärstoffe in Coniferennadeln. PhD thesis, University Köln.

Hrazdina G. 1992. Compartmentation in aromatic metabolism. In: Stafford HA, Ibrahim RK, eds. *Phenolic metabolism in plants*. New York: Plenum Press, 1–23.

Hrazdina G, Marx GA, Hoch HC. 1982. Distribution of secondary plant metabolites and their biosynthetic enzymes in pea (*Pisum sativum* L.) leaves. *Plant Physiology* **70,** 745–8.

Hopp W, Seitz HU. 1987. The uptake of acylated anthocyanin into isolated vacuoles from a cell suspension culture of *Daucus carota*. *Planta* **170,** 74–85.

Ibrahim RK, Barron D. 1989. Phenylpropanoids. In: Dey PM, Harborne JB, eds. *Methods in plant biochemistry*, Vol. 1. *Plant phenolics*. New York: Academic Press, 197–235.

Ibrahim RK. 1992. Immunolocalization of flavonoid conjugates and their enzymes. In: Stafford HA, Ibrahim RK, eds. *Phenolic metabolism in plants*. New York: Plenum Press, 25–61.

Knogge W, Weissenböck G. 1986. Tissue-distribution of secondary phenolic biosynthesis in developing primary leaves of *Avena sativa* L. *Planta* **167,** 196–205.

Markham KR. 1982. *Techniques of flavonoid identification*. (Biological Technique Series), London: Academic Press.

Michel K. 1962. *Die Mikrophotographie*. Wien: Springer-Verlag.

Moskowitz AH, Hradzina G. 1981. Vacuolar contents of fruit subepidermal cells from *Vitis* sp. *Plant Physiology* **68,** 686–92.

Ozimina II. 1979. Flavonoids of *Spartium junceum*. 1. Flavones and flavonols. *Chemistry of Natural Compounds* **16(6),** 763–4.

Polle A, Otter T, Seifert F. 1994. Apoplastic peroxidases and lignification in needles of Norway spruce (*Picea abies* (L.) Karst.). *Plant Physiology* **98,** 53–60.

Reinold S, Hahlbrock K. 1997. *In situ* localization of phenylpropanoid biosynthetic mRNAs and proteins in parsley (*Petroselinum crispum*). *Botanica Acta* **110,** 431–43.

Reuber S, Bornman JF, Weissenböck G. 1996. Phenyl propanoid compounds in primary leaf tissue of rye (*Secale cereale*). Light response of their metabolism and the possible role in UV-B protection. *Physiologia Plantarum* **97,** 160–68.

Rice-Evans CA, Miller NJ, Paganga G. 1997. Antioxidant properties of phenolic compounds. *Trends in Plant Science* **2,** 152–9.

Schmelzer E, Jahnen W, Hahlbrock K. 1988. *In situ* localization of light-induced chalcone synthase mRNA, chalcone synthase and flavonoid endproducts in epidermal cells of parsley leaves. *Proceedings of the National Academy of Sciences*, *USA* **85,** 2989–93.

Schmitz R, Reuber S, Veit M, Weissenböck G. 1996. Comparison of soluble and insoluble hydroxycinnamic acids (HCAs) with soluble flavonoids with regard to UV protection of rye primary leaves. *Plant Physiology and Biochemistry*, Special Issue 1996: 10th FESPP Congress, Florence, 309–10.

Schmutz A, Buchala A, Jenny T, Ryser U. 1994. The phenols in the wax and in the suberin of green cotton fibres and their function. *Acta Horticulturae* **381,** 269–75.

Schnabl H, Weissenböck G, Scharf H. 1986. *In vivo* microspectrophotometric characterisation of flavonol glycosides in *Vicia faba* guard and epidermal cells. *Journal of Experimental Botany* **37,** 61–72.

Schnabl H, Weissenböck G, Sachs G, Scharf H. 1989. Cellular distribution of UV-absorbing compounds in guard and subsidiary cells of *Zea mays* L. *Journal of Plant Physiology* **135,** 249–52.

Schnitzler JP, Jungblut TP, Heller W, Hutzler P, Heinzmann U, Schmelzer E, Ernst D, Langebartels C, Sandermann H. 1996. Tissue localization of UV-B screening pigments and

chalcone synthase mRNA in Scots pine (*Pinus sylvestris* L.) needles. *New Phythologist* **132,** 247–58.

Schulz M, Weissenböck G. 1986. Isolation and separation of epidermal and mesophyll protoplasts from rye primary leaves—tissue-specific characteristics of secondary phenolic product accumulation. *Zeitschrift für Naturforschung* **41c,** 22–7.

Sheahan JJ. 1996. Sinapate esters provide greater UV-B attenuation than flavonoids in *Arabidopsis thaliana* (Brassicaceae). *American Journal of Botany* **83,** 679–86.

Seckmeyer G, Payer HD. 1993. A new sun simulator for ecological research on plants. *Journal of Photochemistry and Photobiology B: Biology* **21,** 175–81.

Sheppard CJR. 1993. Confocal microscopy—principles, practice and options. In: Mason WT, ed. *Fluorescent and luminescent probes for biological activity*. New York: Academic Press, 229–36.

Stober F, Lichtenthaler HK. 1993. Characterization of the laser-induced blue, green and red fluorescence signatures of leaves of wheat and soybroad bean grown under different irradiance. *Physiologia Plantarum* **88,** 696–704.

Strack D, Heilemann J, Klinkott JS. 1988. Cell wall-bound phenolics from spruce needles. *Zeitschrift für Naturforschung* **43c,** 37–41.

Strack D, Keller H, Weissenböck G. 1987. Enzymatic synthesis of hydroxycinnamic acid esters of sugar acids and hydroaromatic acids by protein preparations from rye (*Secale cereale* L.) primary leaves. *Journal of Plant Physiology* **131,** 61–73.

Subhash N, Mazzinghi P, Agati G, Fusi F, Lercari B. 1995. Analysis of laser-induced fluorescence line shape of intact leaves: application to UV stress detection. *Photochemistry and Photobiology* **62,** 711–8.

Thomás-Lorente F, García-Grau MM, Thomás-Barberán FA, Nieto JL. 1989. Acetylated flavonol glycosides from *Vicia faba* leaves. *Phytochemistry* **28,** 1993–5.

Treutter D. 1989. Chemical reaction detection of catechins and proanthocyanins with 4-dimethylamino-cinnamaldehyde. *Journal of Chromatography* **467,** 185–93.

Vierstra RD, John TR, Poff KL. 1982. Kaempferol 3-*O*-galactoside, 7-*O*-rhamnoside is the major green fluorescing compound in the epidermis of *Vicia faba*. *Plant Physiology* **69,** 522–5.

Veit M, Geiger H, Wray V, Abou-Mandour AA, Rozdzinski W, Witte L, Strack D, Czygan F-C. 1993. Equisetumpyrone, a styrylpyrone glucoside in gametophytes from *Equisetum arvense*. *Phytochemistry* **32,** 1029–32.

Veit M, Beckert C, Höhne C, Bauer K, Geiger H. 1995. Interspecific and intraspecific variation of phenolics in the genus *Equisetum* subgenus *Equisetum*. *Phytochemistry* **38,** 881–91.

Vogt T, Pollak P, Tarlyn N, Taylor LP. 1994. Pollination- or wound-induced kaempferol accumulation in petunia stigmas enhances seed production. *Plant Cell* **6,** 11–23.

Wallén P, Carlsson K, Mosberg K. 1992. Properties of confocal microscopy. In: Kriete A, ed. *Visualization in biomedical microscopies*. Weinheim: VCH Verlagsgesellschaft, 109–42.

Weissenböck G, Schnabl H, Sachs H, Elbert C, Heller FO. 1984. Flavonol content of guard cell and mesophyll cell protoplasts isolated from *Vicia faba* L. leaves. *Physiologia Plantarum* **62,** 356–62.

Weissenböck G, Hedrich R, Sachs H. 1986. Secondary phenolic products in isolated guard cell, epidermal cell and mesophyll cell protoplasts—distribution and determination. *Protoplasma* **134,** 141–8.